Dielectronic processes producing radiative stabilization in slow Ne^{10+}+He collisions

J.-Y. Chesnel, H. Merabet, F. Frémont, G. Cremer, X. Husson, D. Lecler, and G. Rieger
Laboratoire de Spectroscopie Atomique—Institut des Sciences de la Matière et du Rayonnement, 6 Bd Maréchal Juin, F-14050 Caen Cedex, France

A. Spieler, M. Grether, and N. Stolterfoht
Hahn-Meitner Institut GmbH, Bereich Festkörperphysik, Glienickerstrasse 100, D-14109 Berlin, Germany
(Received 24 July 1995; revised manuscript received 19 January 1996)

Different contributions to radiative stabilization in Ne^{10+}+He collisions at projectile energies of 10 and 150 keV are studied. For both energies, radiative stabilization is found to be equal to ≈ 0.3 when referred to the total double capture. In Ne^{10+}+He collisions doubly excited states $3lnl'$ and $4lnl'$ ($n \geqslant 4$) are either produced by uncorrelated two-electron transitions or by dielectronic mechanisms due to electron-electron interaction. A strong contribution (≈ 0.15) to the stabilization follows from the decay of near-equivalent electrons $3lnl'$ and $4lnl'$($n=4,5$). Another major contribution (0.10–0.25) to stabilization is due to the decay of configurations $3lnl'$ ($n \geqslant 6$) of nonequivalent electrons produced by the dielectronic process of autoexcitation. A small contribution is found to be due to the configurations $3lnl'$ ($n>9$) created by dielectronic phenomena in the postcollisional and asymptotic regions (≈ 0.04). [S1050-2947(96)06606-1]

PACS number(s): 32.80.Hd, 34.50.Fa

I. INTRODUCTION

In the past few years an increasing interest has been devoted to double-electron capture in slow collisions of multiply charged ions with neutral atomic targets [1–5]. Two-electron transfer results in the creation of doubly excited states due to the configurations $nln'l'$ of the projectile. After the collision, the doubly excited states decay either by Auger electron emission or by photon emission. The photon emission gives rise to the radiative stabilization of the electrons at the projectile ions. Radiative and nonradiative decay processes allow the investigation of the double-capture processes by means of photon spectroscopy [6,7], translational spectroscopy [8], and Auger-electron spectroscopy [1,4,5]. These methods have extensively been used to measure cross sections for populating doubly excited states in many collision systems. Moreover, the mechanisms for radiative stabilization of doubly excited states in few-electron systems have been the subject of several studies and extensive discussions [5,9–13].

For the analysis of radiative stabilization, it is useful to consider two categories of doubly excited configurations $nln'l'$, i.e., involving (near) equivalent electrons ($n \approx n'$) and nonequivalent electrons ($n' \gg n$). (In the following, configurations of near-equivalent electrons are also referred to as equivalent electron configurations.) In the case of equivalent electron configurations, the Auger yield $a_{nln'l'^1L}$, attributed to the state $nln'l'^1L$, is dominant and, hence the related fluorescence yield is rather weak. This has been verified by van der Hart and Hansen [14] for the configurations $3l3l'$ and $3l4l'$ of C^{4+} ions. The situation is quite different for nonequivalent electron configurations which include a core electron and a high-lying Rydberg electron. In this case, due to the small overlap of the corresponding wave functions, the interaction between the electrons is reduced. Therefore the probability for an independent two-electron decay by photon emission becomes considerable. Hence fluorescence yields associated with nonequivalent electron configurations are likely to be significant.

Large fluorescence yields $\omega_{2lnl'}$ have initially been obtained for the radiative transitions from initial states formed by the configurations $2lnl'$ ($n \geqslant 3$) of the ion C^{4+} [5]. For instance, values of $\omega_{2l7l'}$ as large as 0.8 have been found for the configurations $2l7l'$ of the ion C^{4+}. It is emphasized that the creation of these configurations during the collision is caused by the dielectronic process of autoexcitation (AE) involving the transfer of the electrons to high Rydberg states [4,5,15]. Thus it has previously been shown that radiative stabilization plays an important role for double-capture processes into multicharged ions since the population of nonequivalent electron configurations is important [5].

Recently, several experiments have been performed to study other radiative stabilization mechanisms [8,16,17]. Roncin and co-workers [8,17] and Gaboriaud, Roncin, and Barat [16] quoted that radiative-decay branches are relatively large for equivalent electron configurations in many systems. To explain such large contributions to radiative decay, Roncin and co-workers [17] and Bachau, Roncin, and Harel [10] have proposed a postcollisional autoexcitation process, referred to as autotransfer to Rydberg states (ATR), where the two-electron transition occurs at one atomic center. However, these authors found that the experimental values for radiative stabilization are generally higher than those expected from ATR. To understand this finding, Kazansky and Roncin [18] suggested an enhancement of ATR due to the production of Rydberg states with high angular momenta. In this work we will show that other dielectronic processes have to be considered to explain the high amount of radiative stabilization.

It should be noted that in their previous work Roncin and co-workers [17] and Bachau, Roncin, and Harel [10] have systematically neglected other dielectronic processes producing nonequivalent electron configurations. Thus they have given the impression that the postcollisional ATR process is

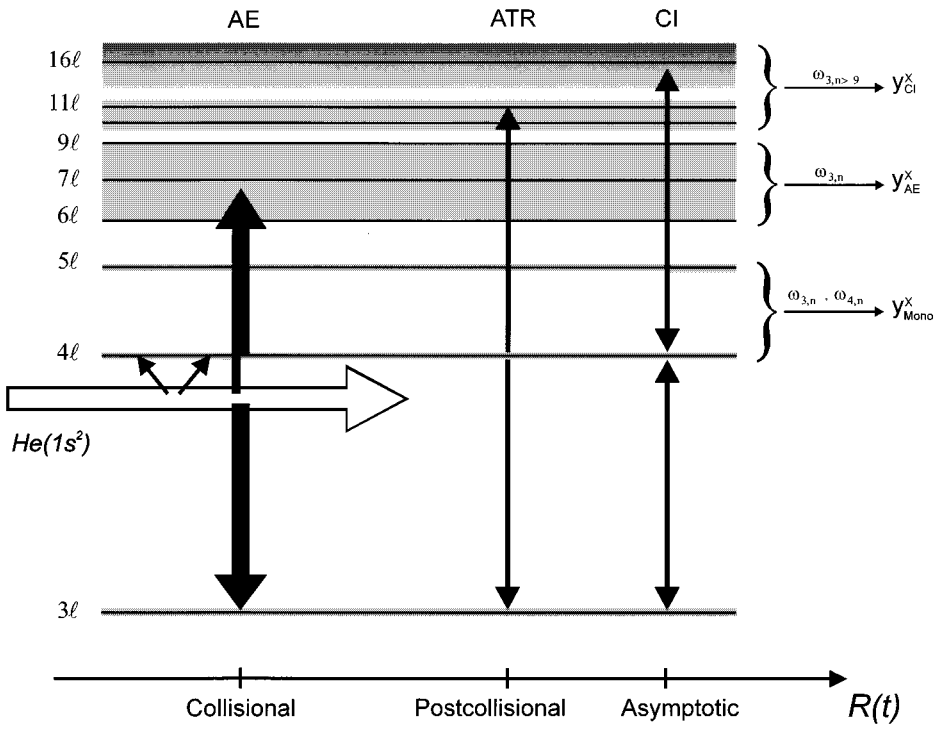

FIG. 1. Diagram of the different contributions to stabilization for the system $Ne^{10+}+He$. Four mechanisms are presented: An uncorrelated two-step process (inclined arrows) and three types of dielectronic processes (vertical arrows). As shown for the case of $4l4l'$, the configurations of equivalent or near-equivalent electrons are dominantly populated by uncorrelated two-step transfers. Configurations of nonequivalent electrons (such as, e.g., $3l6l'$) are created by collisional autoexcitation of the projectile. The configurations $3lnl'$ with $n>9$ are produced either by the postcollisional process ATR or the asymptotic configuration mixing CI. Stabilization originates from the radiative decay of the populated states.

the only mechanism that produces the enhancement of radiative stabilization. However, as previously pointed out by Vaeck and co-workers [19], various dielectronic mechanisms are responsible for the transfer to high Rydberg states. In addition to the collisional autoexcitation process observed previously (15), atomic configuration interaction (CI) of equivalent electrons and nonequivalent electrons may enhance stabilization [9,19,20]. Recently, this latter phenomenon has also been included in the work by Sánchez and Bachau [21].

To provide more insight into the dielectronic processes, in Fig. 1 we depict schematically the mechanisms creating configurations of equivalent and nonequivalent electrons in the system $Ne^{10+}+He$. In the incident channel two electrons occupy the $1s$ orbital of the target He. During the collision, independent two-electron transfers give rise to equivalent electron configurations $4lnl'$ and $3lnl'$ with $n=4$ and 5 at intermediate internuclear distances of typically 5–10 a.u. [15]. In addition, dielectronic processes create the nonequivalent electron configurations $3lnl'$ involving high-lying Rydberg states. These dielectronic mechanisms are rather similar. However, it should be emphasized that characteristic differences occur in the ranges of populated Rydberg states n and the internuclear distances.

First, during the collision the dielectronic process of autoexcitation creates the Rydberg states $3lnl'$ with significant probabilities for n values being in the range from 6 to 9 [15]. Higher Rydberg states ($n>9$) are also produced by AE; however, their populations are small as the corresponding cross sections decrease strongly with increasing n [15]. Second, in the post-collisional region the ATR mechanism produces two-electron transfers from the configurations $4l4l'$ to the Rydberg series $3lnl'$ with n values including the range from about 9 to 12 [21]. The ATR process occurs in the range of internuclear distances from typically 10 to 20 a.u. Moreover, Vaeck and co-workers [19] and van der Hart and Hansen [20] have shown that in the asymptotic region, configuration interaction occurs between $4l4l'$ and $3lnl'$ series with n values being larger than 10. In the following, both ATR and CI are referred to as CI mechanisms since both of them are similar processes of configuration interaction between the states $4l4l'$ and $3lnl'$.

Until today no complete study has been performed to analyze quantitatively the different contributions to radiative stabilization. In the present paper an attempt is made to investigate in detail the different contributions to stabilization in slow $Ne^{10+}+He$ collisions. In particular, the main goal of this work is the comparative study of dielectronic mechanisms which, until now, have been treated rather separately by different groups [9–11]. In this way, our study combines experimental cross sections and theoretical results. The experimental method and the spectra are presented in Sec. II. Then, in Sec. III the total double-capture cross sections and the different contributions to radiative stabilization are evaluated.

Before the data analysis, it is useful to add a few remarks about notations. To date, it became common use to replace the term ''fluorescence yield'' by ''stabilization ratio'' [9,10,17]. We feel that the use of two different terms for the same quantity introduces ambiguities in the study of radiative transition processes. In particular, the attribution of the word ''stabilization'' to individual states or limited number of states appears to be incompatible with its original sense. Therefore we shall use the term ''fluorescence yield'' to denote the radiative branching ratio for individual states. We shall use the notation ''radiative stabilization'' to refer to the mean branching ratio for radiative decay with respect to the *total* number of populated doubly excited states.

II. EXPERIMENTAL METHOD AND SPECTRA ANALYSIS

The experiments at 150 and 10 keV were carried out at the 14-GHz Electron Cyclotron Resonance Ion Sources at

the Grand Accélérateur National d'Ions Lourds (GANIL) in Caen and at Hahn-Meitner Institut (HMI) in Berlin, respectively. At both accelerators we used Auger-spectroscopy apparatus developed at HMI. These apparatus have been described before [22,23] so that only a few details are given here. Ions of 150-keV Ne^{10+} extracted from the ion source were magnetically analyzed and directed into the scattering chamber. The low beam energy of 10 keV was achieved by means of an electrostatic deceleration of the 150-keV ions before entering the scattering chamber. The beam was collimated to a diameter of 2 mm. For the beams of 10 and 150 keV typical currents of about 0.4 and 10 nA, respectively, were collected in a Faraday cup and were used to normalize the spectra. In the scattering chamber, the beam collided a gas-beam target of helium created by an effusive gas jet.

In the present experiments care was taken to maintain single-collision conditions. The average target pressure was estimated to be $\sim 10^{-4}$ mbar. During operation of the gas jet, the residual pressure in the chamber was $\sim 10^{-5}$ mbar, while the base pressure was below 5×10^{-7} mbar. The fraction of charge states other than the primary one present in the incident beam was estimated to be about 15%. For instance, line intensities due to Li-like configurations (i.e., $1s3lnl'$) produced by multiple collisions were observed to be rather small.

Auger electrons created after the collision were measured in a wide range of observation angles including 0° by a tandem electron spectrometer [22,23] which consists of two electrostatic parallel-plate analyzers. The entrance analyzer steered the electrons out of the ion beam and suppressed background electrons. The exit analyzer determined the energy of the electrons with high resolution. The intrinsic resolution of the exit analyzer was 5% within the full width at half maximum (FWHM). A constant energy resolution of 1.5 eV was achieved by decelerating the electrons in the region between the analyzers, to 30 eV.

Figure 2 shows typical L-Auger spectra obtained for projectile energies of 10 and 150 keV. The observation angle is 40° with respect to the incident beam direction. The peaks are attributed to the configurations $3lnl'$ with $n=4$–9. The line group centered at 180 eV is associated with the configurations $4l4l'$ and the series limit of the configurations $3lnl'$, which decay to the $2l\epsilon l'$ continuum by means of Auger transitions. Auger electrons from the configurations $4lnl'$ ($n=5$–6) have also been observed in the present experiment. The associated peaks due to M-Auger transitions are observed in the electron-energy range from 20 to 50 eV. The $4l7l'$ Auger intensity is barely visible in the spectra.

To evaluate absolute cross sections from the observed electron spectra (Fig. 2), we used methods described previously [22]. First, the measured Auger spectra were integrated to determine single-differential cross sections $d\sigma^a_{n,n'}/d\Omega$ for Auger-electron emission attributed to a given complex n/n'. Moreover, total cross sections for Auger-electron emission $\sigma^a_{n,n'}$ were evaluated by integration of $d\sigma^a_{n,n'}/d\Omega$ over the electron-emission angle. The results are given in Table I. The absolute uncertainties for the evaluated cross sections are about 30% and the relative uncertainties with respect to a variation of the emission angle are 20%. The experimental data were used to determine total double-capture cross sections $\sigma_{n,n'}$ by dividing $\sigma^a_{n,n'}$ by the corresponding average Auger yield $a_{n,n'}$ calculated theoretically. The obtained double-capture cross sections are given in Table II.

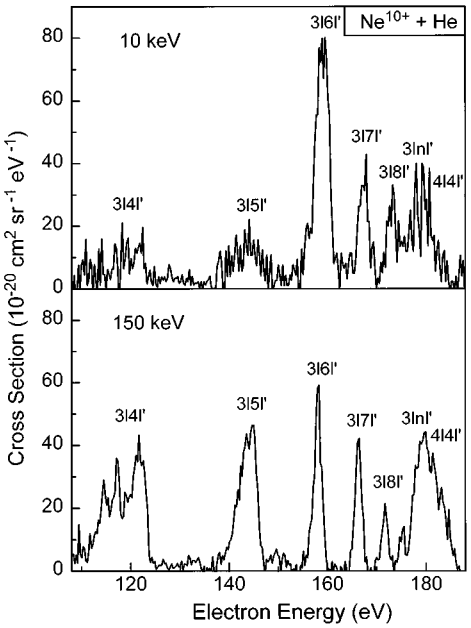

FIG. 2. High-resolution spectra of L-shell Auger electrons produced in Ne^{10+}+He collisions at projectile energies of 10 and 150 keV. Each peak corresponds to the Auger decay of states associated with a configuration $3lnl'$ ($n=4$–9). The peak centered at 180 eV corresponds to the limit of the $3lnl'$ series and to the configurations $4l4l'$ which decay to the $2l\varepsilon l'$ configurations.

The calculations of the average Auger yields are presented in Ref. [24]. Also, the principle of the theoretical method has been discussed in detail by Stolterfoht *et al.* [5] so that only a brief description is given here. Using the Hartree-Fock code by Cowan [25], radiative and nonradiative decay rates for the states $|nln'l'\gamma J_\gamma\rangle$ [26] were evaluated to determine the associated individual Auger yields $a_{nln'l'\gamma J_\gamma}$. The average L- and M-Auger yields for the configurations $3lnl'$ ($n=4$–9) and $4lnl'$ ($n=4$–6), respectively, were obtained by means of the expression

$$a_{n,n'}=\sum_{l,l',\gamma,J} Q_{n,n'}(l,l',\gamma,J_\gamma)a_{nln'l'\gamma J_\gamma}, \tag{1}$$

where $Q_{n,n'}(l,l',\gamma,J_\gamma)$ is the probability for the production of the state $|nln'l'\gamma J_\gamma\rangle$. A simple model was adopted in which this probability is factorized [5,24],

$$Q_{n,n'}(l,l',\gamma,J_\gamma)=q_n(l)q_{n'}(l')p(J_\gamma)s(\gamma), \tag{2}$$

where $q_n(l)$, $q_{n'}(l')$, and $p(J_\gamma)$ are the occupation probabilities associated with the quantum numbers l, l', and J_γ, respectively, and $s(\gamma)$ is the squared coefficient of the singlet component of the intermediate coupling state γ.

For details of the calculations of $q_n(l)$, $q_{n'}(l')$, $p(J_\gamma)$, and $s(\gamma)$ the reader is referred to Refs. [5,24]. The probability $p(J_\gamma)$ was obtained by assuming a statistical population of the state specified by the total angular momentum J_γ. The probabilities $q_n(l)$ and $q_{n'}(l')$ were estimated using the

TABLE I. Total Auger-electron emission cross sections $\sigma^a_{n,n'}$ measured for the configurations of doubly excited states $3lnl'$ and $4lnl'$ ($n \geq 4$) produced in 10- and 150-keV Ne^{10+}+He collisions. The experimental uncertainties are about 20% (see text). The corresponding Auger yields $a_{n,n'}$ and fluorescence yields $\omega_{n,n'}$, which were previously calculated by means of the Cowan code [24], are also given. The average Auger yields $a_{n,n'}$ are compared with those $a^{VH}_{n,n'}$ given by van der Hart, Vaeck, and Hansen [29,30].

Configurations	$\sigma^a_{n,n'}$ (10^{-17} cm^2)				
$nln'l'$	10 keV	150 keV	$a_{n,n'}$	$a^{VH}_{n,n'}$	$\omega_{n,n'}$
$3l4l'$	1.25±0.25	4.07±0.81	0.75		0.25
$3l5l'$	1.32±0.26	2.99±0.60	0.67		0.33
$3l6l'$	3.77±0.75	1.50±0.30	0.60		0.40
$3l7l'$	1.32±0.26	1.02±0.20	0.56	0.59 [a]	0.44
$3l8l'$	0.88±0.18	0.50±0.10	0.52	0.48 [a]	0.48
$3l9l'$	0.44±0.09	0.33±0.07	0.47	0.43 [a]	0.53
$3lnl'$ ($n>9$)	0.44±0.09	0.41±0.08	0.45		0.55
180-eV peak	1.37±0.27	3.61±0.72			
$4l5l'$	3.64±0.73	9.80±1.96	0.91	0.94	0.09
$4l6l'$	0.87±0.17	2.35±0.47	0.79		0.21

[a]See Ref. [30].

model by Burgdörfer, Morgenstern, and Niehaus [27]. In accordance with experimental results of Meyer *et al.* [28], the population of high-angular-momentum states was included in the distribution $q_{n'}(l')$. It is emphasized that the variation of $q_n(l)$ and $q_{n'}(l')$ with respect to the collision energy was found to be weak in the investigated range from 10 to 150 keV. Furthermore, the average Auger yields $a_{n,n'}$ were found to be rather insensitive to the distributions $q_n(l)$ and $q_{n'}(l')$ [24]. Hence in contrast to the suggestion of Kazansky and Roncin [18] we concluded that the choice of the distributions $q_n(l)$ and $q_{n'}(l')$ is uncritical for the determination of the average Auger yields $a_{n,n'}$ [24].

It is of particular interest to compare the calculated Auger yields with the most accurate *ab initio* calculations performed by van der Hart, Vaeck, and Hansen [29,30]. First, a comparison between the individual Auger yields $a_{nln'l'\gamma J_\gamma}$ and results given by van der Hart and co-workers [29,30] for the singlet states $4l5l'$ shows good agreement [24]. For the present analysis, we determined average Auger yields for which the uncertainties of individual $a_{nln'l'\gamma J_\gamma}$ are smoothed out. In Table I, typical average Auger yields $a_{n,n'}$ are compared with the calculations performed by a B-spline-based method [29,30]. Good overall agreement is obtained between the two sets of methods. The differences between the corresponding Auger yields are smaller than 10%. It is therefore reasonable to invoke an uncertainty of about 10% for the average Auger yields used in this work. Since the experimental uncertainties are as large as 20%, the uncertainties for the average Auger (and fluorescence) yields provide a small contribution to the uncertainties for the double-capture cross sections and hence play an unimportant role for the following conclusions.

TABLE II. Total double-electron-capture cross sections $\sigma_{n,n'}$ obtained for the configurations of doubly excited states $3lnl'$ and $4lnl'$ ($n \geq 4$) produced in 10- and 150-keV Ne^{10+}+He collisions. For the evaluation of the double-capture cross sections attributed to the configurations $3lnl'$ ($n>9$) and $4l4l'$ see Sec. II. At the bottom of the table, the total cross section $\sigma_{\rm tot}$ including all double-capture states is given for the collision energies of 10 and 150 keV.

Configurations	$\sigma_{n,n'}$ (10^{-17} cm^2)	
$nln'l'$	10 keV	150 keV
$3l4l'$	1.66±0.42	5.43±1.36
$3l5l'$	1.97±0.49	4.46±1.12
$3l6l'$	6.28±1.57	2.52±0.63
$3l7l'$	2.36±0.59	1.82±0.46
$3l8l'$	1.69±0.42	0.96±0.24
$3l9l'$	0.93±0.23	0.71±0.18
$3lnl'$ ($n>9$)	0.97±0.24	0.92±0.23
$4l4l'$	1.47±0.36	5.08±1.27
$4l5l'$	4.00±1.00	10.76±2.69
$4l6l'$	1.10±0.28	2.97±0.74
$\sigma_{\rm tot}$ (10^{-17} cm^2)	22.43±5.61	35.63±8.91

After the determination of the average Auger yields, we focused attention on the configuration interaction between $4l4l'$ and $3lnl'$ ($n>9$). The spectrum peak centered at 180 eV (Fig. 2) was integrated to determine the total cross section $\sigma^a_{(180\ \rm eV)}$ for Auger-electron emission from the configurations $4l4l'$ and $3lnl'$ with $n>9$. The cross section $\sigma^a_{(180\ \rm eV)}$ is a summation over three different Auger-emission contributions as follows:

$$\sigma^a_{(180\ \rm eV)} = \sigma_{3,n>9} a_{3,n>9} + \sigma_{4,4}\tau a_{3,n>9} + \sigma_{4,4}(1-\tau)a_{4,4}\,. \tag{3}$$

In this summation, the term $\sigma_{3,n>9}a_{3,n>9}$ accounts for the Auger-emission cross section for the configurations $3lnl'$ ($n>9$) created by the collisional autoexcitation process. The corresponding double-capture cross section $\sigma_{3,n>9}$ summed over n was estimated by means of an extrapolation by fitting the function $n^{-\alpha}$ to the intensities of the states $3lnl'$ with

TABLE III. Contributions to radiative stabilization of doubly excited Ne^{8+} ions originating from the 10- and 150-keV $Ne^{10+}+He$ collisions. These contributions y^X are due to the decay of the doubly excited states $nln'l$ which are produced by the different mechanisms. In the first column, the label ''mono'' refers to mechanisms involving monoelectronic processes and AE and CI refer to dielectronic processes. In the last row, the fraction S of ions Ne^{8+} which stabilize radiatively with respect to the total number of doubly excited ions Ne^{8+} is given.

Mechanisms	Configurations $nln'l'$	Contributions to stabilization y^X 10 keV	150 keV
mono	$3lnl'$ ($n=4$–5) and $4lnl'$ ($n=4$–6)	0.08±0.02	0.14±0.04
AE	$3lnl'$ ($n\geqslant 6$)	0.24±0.07	0.09±0.03
CI	$4l4l'\rightarrow 3lnl'$ ($n>9$)	0.02±0.01	0.05±0.02
Stabilization S		0.34±0.10	0.28±0.09

$n=6$–9. The double-capture cross sections for $n>9$ were found to be small in comparison with the cross section associated with $4l4l'$ (Table II).

In Eq. (3), the term $\sigma_{4,4}\tau a_{3,n>9}$ refers to the total cross section for Auger emission from the Rydberg components $3lnl'$ ($n>9$) created by both postcollisional and asymptotic CI mechanisms. The quantity $\sigma_{4,4}$ is the total cross section for producing the doubly excited states $4l4l'$ in the collisional region. The quantity τ refers to the total fraction of the initial $4l4l'$ population which dilutes into the nonequivalent electron configurations $3lnl'$ by CI processes.

Hence the last term of the summation in Eq. (3), i.e., $\sigma_{4,4}(1-\tau)a_{4,4}$, accounts for Auger-electron emission from the components $4l4l'$. The average Auger yield $a_{4,4}$ was found to be 0.9 [30]. From the results obtained for cross sections $\sigma^a_{(180\ \mathrm{eV})}$ and $\sigma_{3,n>9}$, the double-capture cross section $\sigma_{4,4}$ for producing the doubly excited state $4l4l'$ in the collisional region was determined by means of Eq. (3).

Recently, Sánchez and Bachau [21,31] have studied the CI mechanisms in the case of doubly excited ions Ne^{8+}. They found that the fraction τ is equal to ~ 0.6. We consider this number as an upper limit estimate for the postcollisional and asymptotic mechanisms of configuration interaction.

III. RESULTS AND DISCUSSION

Table II gives the results for the total double-capture cross sections obtained for the collisions $Ne^{10+}+He$ at impact energies of 10 and 150 keV. It is seen that the cross sections for producing the configurations of near-equivalent electrons $3lnl'$ and $4lnl'$ ($n=4,5$) are dominant for 150 keV, whereas they decrease at 10 keV. On the contrary, the production of the nonequivalent electron configurations $3lnl'$ with n values ranging from 6 to 9 increases significantly at 10 keV. At this energy, the production of nonequivalent electron states becomes as large as that of near-equivalent electron states. As noted above, the observed high Rydberg states $3lnl'$ ($n=6$–9) are predominantly produced in the collisional region at internuclear distance of typically 5 a.u. Thus our study provides experimental evidence for the fact that the nonequivalent electron configurations $3lnl'$ created by the collisional autoexcitation play a significant role for radiative stabilization.

The different contributions to stabilization with respect to the total double-capture cross section were based on the experimental cross sections given in Table II. The contributions are denoted by letters indicated in Fig. 1: The quantity y^X_{mono} refers to the contribution which follows from the decay of the near-equivalent electron configurations $3lnl'$ ($n=4$–5) and $4lnl'$ ($n=4$–6) mainly produced by monoelectronic processes. The contribution originating from the decay of the nonequivalent electron configurations $3lnl'$ ($n=6$–9) created by the dielectronic process AE is referred to as y^X_{AE}. The quantity y^X_{CI} is the contribution to stabilization due to photon emission from the high Rydberg states $3lnl'$ produced in the postcollisional and asymptotic regions:

$$y^X_{\mathrm{mono}}=\frac{\sigma_{n,n'}\omega_{n,n'}}{\sigma_{\mathrm{tot}}}, \tag{4}$$

$$y^X_{\mathrm{AE}}=\frac{\sigma_{3,n}\omega_{3,n}}{\sigma_{\mathrm{tot}}}, \tag{5a}$$

$$y^X_{\mathrm{CI}}=\frac{\sigma_{4,4}\tau\omega_{3,n>9}}{\sigma_{\mathrm{tot}}}, \tag{5b}$$

where σ_{tot} is the total cross section including all double-capture states and $\omega_{n,n'}$ is the average fluorescence yield associated to a given configuration $nln'l'$ summed over l and l' (Tables I and II). Equation (4) refers to the uncorrelated two-electron transfers and Eq. (5) to the dielectronic processes. It is pointed out here that the radiative stabilization is given by the sum of the individual contributions as

$$S=y^X_{\mathrm{mono}}+y^X_{\mathrm{AE}}+y^X_{\mathrm{CI}}. \tag{6}$$

The results obtained for the different contributions to radiative stabilization are given in Table III and shown in Fig. 3. The radiative stabilization value S of the doubly excited system $Ne^{10+}+He$ is found to be about 0.30 for the impact energies of 10 and 150 keV. Within the experimental uncertainties, the present stabilization values S agree with recent measurements performed by means of recoil ion spectroscopy [32,33].

The contribution to radiative stabilization due to equivalent electron configurations is found to be of the same order of magnitude as the contribution attributed to nonequivalent electron configurations. In the case of 150-keV $Ne^{10+}+He$ collisions, the decay of equivalent electron configurations provides the largest contribution to radiative stabilization.

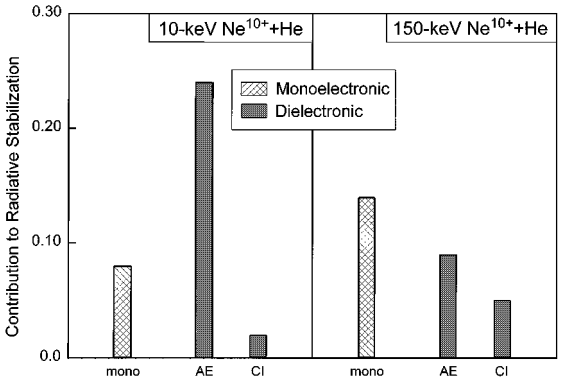

FIG. 3. Contributions to stabilization originating from radiative decay of doubly excited states produced by monoelectronic and dielectronic processes in 10- and 150-keV $Ne^{10+}+He$ collisions. The label ''mono'' denotes the contribution associated with the uncorrelated processes dominantly responsible for the production of equivalent electron configurations $3lnl'$ $(n=4–5)$ and $4lnl'$ $(n=4–6)$ during the collision. The labels AE and CI refer to the dielectronic processes responsible for the creation of nonequivalent electron configurations $3lnl'$ in the collisional region, and postcollisional and asymptotic regions, respectively.

The contribution associated with the equivalent electron states is still significant at 10 keV (~ 0.1) (Table III). Furthermore, although the fluorescence yield $\omega_{4,4}$ (~ 0.1) [29,30] is nearly equal to $\omega_{4,5}$, the $4l4l'$ contribution to stabilization is found to be smaller than that for $4l5l'$. This is due to the fact that the cross section for producing the states $4l5l'$ is dominant in the group of equivalent electron configurations.

Next, we consider the dielectronic mechanisms producing configurations of nonequivalent electrons. At both energies of 10 and 150 keV a significant contribution to stabilization originates from the configurations $3lnl'$ $(n \geqslant 6)$ created by the collisional process of autoexcitation. The remarkable feature is that this AE contribution increases strongly with decreasing projectile velocity so as to become the major contribution to stabilization (0.24) at the collision energy of 10 keV. On the contrary, as depicted in Fig. 3, the decay of configurations $3lnl'$ $(n>9)$ due to postcollisional and asymptotic CI processes gives rise to the smallest contribution to stabilization, in particular at the projectile energy of 10 keV.

Our analysis shows that the major contribution to stabilization originates from the states $3lnl'$ with $n \geqslant 4$ which are populated during the collision at internuclear distances of typically 5 a.u. (Fig. 3 and Table III). This is in disagreement with the results obtained by Roncin and co-workers [17], who quoted that the population of the states $3lnl'$ during the collision is negligible. These authors stated that uniquely the equivalent electron configurations $4l4l'$ and $4l5l'$ are produced in 10-keV $Ne^{10+}+He$ collisions. Then, they supposed that the postcollisional and asymptotic mechanisms play the major role for the radiative stabilization. In view of our results, their conclusions above the different contributions to stabilization are incorrect.

Recent Auger-electron spectra measured by Bordenave-Montesquieu *et al.* [34] clearly showed that the configurations $3lnl'$ with $n \geqslant 5$ are strongly populated in 100-keV $Ne^{10+}+He$ collisions. Unfortunately, the above authors assumed that the fluorescence yields $\omega_{3,n}$ are equal to zero for $n \leqslant 9$ and become significantly large for $n>9$. Their assumptions disagree with our calculated results obtained for $\omega_{3,n}$ [24] (see also Table I). Hence, like Roncin and co-workers [17], they gave the erroneous impression that the dominant contribution to stabilization originates from the decay of Rydberg components $3lnl'$ $(n>9)$ created in the postcollisional region.

Configuration-interaction processes give rise to an enhancement of the $4l4l'$ contribution to stabilization since they create components $3lnl'$ (with $n>9$) which decay noticeably by photon emission. For instance, the fluorescence yield $\omega_{4,4}$ was recently found to be about 0.1 when neglecting the CI processes [30]. When the configuration interaction between the states $4l4l'$ and $3lnl'$ $(n>9)$ is taken into account, this fluorescence yield becomes as large as 0.25–0.35 [29,35,36]. It should be realized, however, that this increase of the fluorescence yield plays a minor role in the total balance of stabilization. The cross section for producing the doubly excited state $4l4l'$ is found to be rather small in comparison with the $4l5l'$ and $3lnl'$ cross sections (Table II). Thus the decay of components $3lnl'$ produced by CI contributes weakly to the stabilization process.

IV. CONCLUSION

In this work we report on the mechanisms responsible for the production of radiative stabilization in the collision system $Ne^{10+}+He$ at impact energies of 10 and 150 keV. The attempt was made to provide a complete quantitative study of the stabilization phenomenon including monoelectronic and dielectronic effects in the electron transfer mechanisms. The different contributions to stabilization were extracted from experimental double-capture cross sections and theoretical results for branching ratios [15,21,24]. It is shown that the double electron capture into the states associated with the configurations $3lnl'$ $(n \geqslant 4)$ of equivalent and nonequivalent electrons plays a major role in the stabilization process.

On the contrary, the contribution originating from the radiative decay of the configurations $4l4l'$ was found to be rather small in comparison with the $4l5l'$ and $3lnl'$ contributions. Nevertheless, specific attention was devoted to the decay of the configurations $4l4l'$, since they have been shown to interact significantly with the Rydberg configurations $3lnl'$ $(n>9)$ [20,21]. Sánchez and Bachau [21,31] have found that the total probability of population of states $3lnl'$ due to postcollisional and asymptotic mechanisms is as large as 0.60. However, the decay of high Rydberg states created in postcollisional and asymptotic regions by CI gives rise to stabilization whose contribution does not exceed 0.05. For example, the CI contribution is about ten times smaller than the contribution attributed to the autoexcitation process producing the configurations $3lnl'$ during the collision at 10 keV.

For the determination of the average fluorescence and Auger yields, we used different occupation probabilities that were estimated in an approximative manner [24]. However, these probabilities are found to depend only slightly on the collision energy and they do not influence critically the fluorescence yields. Therefore the major conclusions of the

present study are not affected by the uncertainties of the fluorescence and Auger yields.

The present work provides clear evidence that the role of the dielectronic autoexcitation process, which occurs during the collision, is substantial for the production of nonequivalent electron configurations and for radiative stabilization. It is evident that in future experimental and theoretical studies the major contributions to radiative stabilization must be adequately taken into account.

ACKNOWLEDGMENTS

We are grateful to Alain Lepoutre for providing the data-acquisition computer program. We are much indebted to the staffs of the ECR sources in Berlin and Caen for their generous assistance. We would like to thank N. Vaeck, J. E. Hansen, H. W. van der Hart, and H. Bachau for fruitful discussions and for providing us with their results prior to publication. This work was supported by the European Collaboration Research Program PROCOPE.

[1] M. Boudjema, M. Cornille, J. Dubau, P. Moretto-Capelle, A. Bordenave-Montesquieu, P. Benoit-Catin, and A. Gleizes, J. Phys. B **24**, 1713 (1991).

[2] N. Stolterfoht, C. C. Havener, R. A. Phaneuf, J. K. Swenson, S. M. Shafroth, and F. W. Meyer, Phys. Rev. Lett. **57**, 74 (1986).

[3] A. Niehaus, J. Phys. B **19**, 1925 (1986).

[4] F. Frémont, K. Sommer, D. Lecler, S. Hicham, P. Boduch, X. Husson, and N. Stolterfoht, Phys. Rev. A **46**, 222 (1992).

[5] N. Stolterfoht, K. Sommer, J. K. Swenson, C. C. Havener, and F. W. Meyer, Phys. Rev. A **42**, 5396 (1990).

[6] S. Bliman, J. J. Bonnet, D. Hitz, T. Ludcec, M. Druetta, and M. Mayo, Nucl. Instrum. Methods Phys. Res. Sect. B **27**, 579 (1987).

[7] D. Vernhet, A. Chetioui, J. P. Rozet, C. Stephan, K. Wohrer, A. Touati, M. F. Politis, P. Bouisset, D. Hitz, and S. Dousson, J. Phys. B **22**, 1603 (1989).

[8] P. Roncin, M. N. Gaboriaud, and M. Barat, Europhys. Lett. **16**, 551 (1991).

[9] H. W. van der Hart, N. Vaeck, and J. E. Hansen, J. Phys. B **27**, 3489 (1994).

[10] H. Bachau, P. Roncin, and C. Harel, J. Phys. B **25**, L109 (1992).

[11] N. Stolterfoht, Phys. Scr. **T51**, 39 (1994).

[12] H. Merabet, F. Frémont, J.-Y. Chesnel, G. Cremer, X. Husson, D. Lecler, A. Lepoutre, G. Rieger, and N. Stolerfoht, Nucl. Instrum. Methods Phys. Res. Sect. B **99**, 75 (1995).

[13] J. P. Desclaux, Nucl. Instrum. Methods Phys. Res. Sect. B **98**, 18 (1995).

[14] H. W. van der Hart and J. E. Hansen, J. Phys. B **26**, 641 (1993).

[15] F. Frémont, H. Merabet, J.-Y. Chesnel, X. Husson, A. Lepoutre, D. Lecler, and N. Stolterfoht, Phys. Rev. A **50**, 3117 (1994).

[16] M. N. Gaboriaud, P. Roncin, and M. Barat, J. Phys. B **26**, L303 (1993).

[17] P. Roncin, M. N. Gaboriaud, Z. Szilagyi, and M. Barat, *Proceedings of the XVIII International Conference on the Physics of Electronic and Atomic Collisions, Aarhus, Denmark, 1993*, edited by T. Andersen, B. Fastrup, F. Folkmann, J. Knudsen, and N. Andersen, AIP Conf. Proc. No. 295 (AIP, New York, 1993), p. 537.

[18] A. K. Kazansky, J. Phys. B **25**, L381 (1992); A. K. Kazansky and P. Roncin, *ibid.* **27**, 5537 (1994).

[19] N. Vaeck and J. E. Hansen, J. Phys. B **26**, 2977 (1993); N. Vaeck, H. W. van der Hart, and J. E. Hansen, in Ref. [17], p. 794.

[20] H. W. van der Hart and J. E. Hansen, J. Phys. B **27**, L395 (1994).

[21] I. Sánchez and H. Bachau, J. Phys. B **28**, 795 (1995).

[22] N. Stolterfoht, Z. Phys. **248**, 81 (1971); **248**, 92 (1971).

[23] A. Itoh, T. Schneider, G. Schiwietz, Z. Roller, H. Platten, G. Nolte, D. Schneider, and N. Stolterfoht, J. Phys. B **16**, 3965 (1983).

[24] H. Merabet, G. Cremer, F. Frémont, J.-Y. Chesnel, and N. Stolterfoht, Phys. Rev. A (to be published).

[25] R. D. Cowan, *The Theory of Atomic Structure and Spectra* (University of California Press, Berkeley, 1981).

[26] The calculations were performed for two-electron states $|nln'l'\gamma J_\gamma\rangle$, where J_γ is the total angular momentum and γ labels the states obtained within the framework of the intermediate coupling scheme.

[27] J. Burgdörfer, R. Morgenstern, and A. Niehaus, J. Phys. B **19**, L507 (1987).

[28] F. W. Meyer, D. C. Griffin, C. C. Havener, M. S. Huq, R. A. Phaneuf, J. K. Swenson, and N. Stolterfoht, Phys. Rev. Lett. **60**, 1821 (1988).

[29] H. W. van der Hart, N. Vaeck, and J. E. Hansen, J. Phys. B **28**, 5207 (1995).

[30] J. E. Hansen, N. Vaeck, and H. W. van der Hart (private communication).

[31] H. Bachau (private communication).

[32] S. Martin, J. Bernard, L. Chen, A. Denis, and J. Désesquelles, Phys. Rev. A **52**, 1218 (1995).

[33] S. Duponchel, A. Cassimi, P. Jardin, D. Hennecart, and X. Fléchard (private communication).

[34] A. Bordenave-Montesquieu, P. Moretto-Capelle, A. Gonzalez, M. Benhenni, H. Bachau, and I. Sánchez, J. Phys. B **27**, 4243 (1994).

[35] H. Bachau and I. Sánchez, Nucl. Instrum. Methods Phys. Res Sect. B **98**, 78 (1995).

[36] The value of about 0.35 is obtained by calculating the summation $(1-\tau)\omega_{4,4}+\tau\omega_{3,n>9}$ where τ is chosen to be equal to the maximum value of ≈ 0.6. Hence the number of 0.35 is an upper limit estimate of the fluorescence yield associated with the mixed asymptotic doubly excited state including components $4l4l'$ and $3lnl'$ $(n>9)$. In particular, this number is slightly larger than the value of 0.3 given by van der Hart, Vaeck, and Hansen [29].